

AD-A102 840

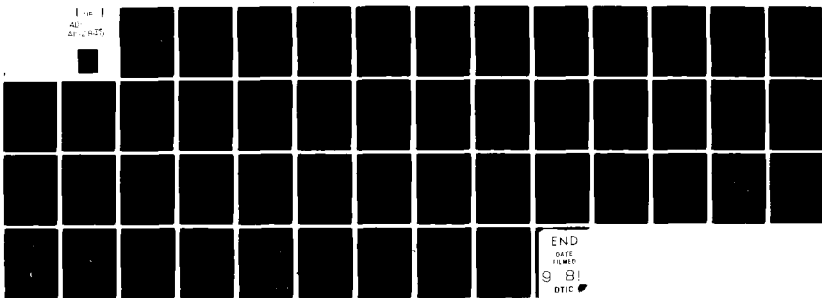
BROWN UNIV. PROVIDENCE RI DEPT OF CHEMISTRY  
RAMAN SPECTROSCOPIC STUDY OF MOLECULAR ORIENTATION IN VITREOUS

F/G 11/2  
--ETC(U)  
N00014-75-C-0883  
NL

JUL 81 C F WINDISCH, W M RISEN

UNCLASSIFIED TR-81-01

Line 1  
AD-  
AD-A102 840



END  
DATE  
FILED  
9 81  
DTIC

AD A102840

12

OFFICE OF NAVAL RESEARCH

Contract ONR-A00014-75-C-0883/NR-051-539

TECHNICAL REPORT NO. TR-81-01

LEVEL 12

Raman Spectroscopic Study of Molecular Orientation in Vitreous  $\text{B}_2\text{O}_3$  Films

by

Charles F. Windisch and William M. Risen, Jr.

Prepared for Publication  
in the  
Journal of Non-crystalline Solids

July 10, 1981

164  
S DTIC ELECTED AUG 14 1981  
E

Department of Chemistry  
Brown University  
Providence, R.I. 02912

July 10, 1981

Reproduction in whole or in part is permitted for  
any purpose of the United States Government

Approved for Public Release; Distribution Unlimited

DNC FILE COPY

81 8 14 060

SECURITY CLASSIFICATION OF THIS PAGE (When Data Entered)

REPORT DOCUMENTATION PAGE		READ INSTRUCTIONS BEFORE COMPLETING FORM
1. REPORT NUMBER TR-81-01	2. GOVT ACCESSION NO. AD-H102	3. RECIPIENT'S CATALOG NUMBER 840
4. TITLE (and Subtitle) Raman Spectroscopic Study of Molecular Orientation in Vitreous B <sub>2</sub> O <sub>3</sub> Films	5. TYPE OF REPORT & PERIOD COVERED Technical	
6. AUTHOR(s) Charles F. Windisch and William M. Risen, Jr.	7. CONTRACT OR GRANT NUMBER(s) N00014-75-C-0883 NR-051-539	
8. PERFORMING ORGANIZATION NAME AND ADDRESS Department of Chemistry Brown University Providence, Rhode Island 02912	9. PROGRAM ELEMENT, PROJECT, TASK AREA & WORK UNIT NUMBERS	
10. CONTROLLING OFFICE NAME AND ADDRESS Office of Naval Research United States Navy	11. REPORT DATE July 10, 1981	
12. MONITORING AGENCY NAME & ADDRESS (if different from Controlling Office)	13. NUMBER OF PAGES 41	
14. SECURITY CLASS (of this report)	15. DECLASSIFICATION/DOWNGRADING SCHEDULE	
16. DISTRIBUTION STATEMENT (of this Report) Distribution Unlimited; Approved for Public Release	17. DISTRIBUTION STATEMENT (of the abstract entered in Block 20, if different from Report)	
18. SUPPLEMENTARY NOTES		
19. KEY WORDS (Continue on reverse side if necessary and identify by block number) glass, Raman spectra, molecular orientation, B <sub>2</sub> O <sub>3</sub> , glass film, boroxol ring, glass structure, boron oxide		
20. ABSTRACT (Continue on reverse side if necessary and identify by block number) Preferred orientation of a molecular unit in vitreous B <sub>2</sub> O <sub>3</sub> films prepared under tensile stress is demonstrated by laser Raman spectroscopy. The polarized Raman scattering is reported and found to be strongly dependent on sample orientation and polarization of the incident and scattered light. The ratios of scattering intensities in the various scattering arrangements for films are substantially different from those for bulk B <sub>2</sub> O <sub>3</sub> (g1). Calculated Raman intensity ratios based upon the proposed oriented boroxol ring structure compare well with		

the experimental values. These results demonstrate the tendency of a molecular unit with the properties of a boroxol ring to become preferentially oriented in response to an applied stress, and provide evidence for the existence of boroxol rings in  $B_2O_3$ (gl).

Accession For	
NTIS	REF ID:
DTIC	DA
Unclassified	
Justified	
By	
Distribution	
Availability Status	
Dist	Avail. Off/Or Specifi
A	

Raman Spectroscopic Study of Molecular Orientation in Vitreous  $B_2O_3$

Films

Charles F. Windisch and William M. Risen, Jr.

Department of Chemistry  
Brown University  
Providence, Rhode Island 02912

Abstract

Preferred orientation of a molecular unit in vitreous  $B_2O_3$  films prepared under tensile stress is demonstrated by laser Raman spectroscopy. The polarized Raman scattering is reported and found to be strongly dependent on sample orientation and polarization of the incident and scattered light. The ratios of scattering intensities in the various scattering arrangements for films are substantially different from those for bulk  $B_2O_3$  (gl). Calculated Raman intensity ratios based upon the proposed oriented boroxol ring structure compare well with the experimental values. These results demonstrate the tendency of a molecular unit with the properties of a boroxol ring to become preferentially oriented in response to an applied stress, and provide evidence for the existence of boroxol rings in  $B_2O_3$  (gl).

Introduction

It has been proposed widely that vitreous  $B_2O_3$  is composed principally of interconnected boroxol ( $B_3O_3$ ) rings (1-10). The postulated boroxol structure, shown in Fig. 1, is planar and has  $D_{3h}$  point group symmetry. The planarity of the boroxol ring structure distinguishes it from other possible clusters, or ways of connecting,  $BO_3$ -triangles, and serves to allow the  $BO_3$ -triangles, whose presence is consistent with  $^{11}B$ -NMR findings (9), to exist in an intermediate range pseudomolecular unit.

The vibrational spectra of  $^{18}O$ -isotopically labelled  $B_2O_3$ (gl),  $B_2^{16}O_3$ (gl), and mixed isotope  $B_2O_3$ (gl) support the postulate that boroxol rings constitute a dominant structural feature of  $B_2O_3$ (gl) (11). From that study it is also clear that the main Raman-active band of  $B_2O_3$ (gl) assigned to the boroxol ring, observed at  $808\text{ cm}^{-1}$  in  $B_2^{16}O_3$ (gl), is not strongly coupled to the interconnecting network. This band is strong and relatively narrow, and in bulk samples it is highly polarized.

There have been alternative proposals for the structure which do not involve the boroxol ring, or, indeed, any intermediate range order. Thus, Elliott concluded that the observed X-ray diffraction radial distribution function can be computed at least as well by assuming a continuous random network (CRN) of planar  $BO_3$ -units (12). Galeener, Lucovsky and Mikkelsen (10), in reporting their vibrational spectra, also have pointed out the inconsistency of conflicting interpretations of the X-ray data, and examined the feasibility of interpreting the spectra on the basis of the CRN model. Moreover, Soules and Varshneya (26) reported that their molecular dynamic calculations on  $B_2O_3$  do not indicate boroxol ring formation if no

directional bonding is included in the potential function.

If the boroxol ring structure does exist in vitreous  $B_2O_3$  and in the melt (or at least the material in the transformation range), it is a unit which should respond to an applied mechanical stress in a predictable manner.

When material is subjected to an applied stress, the structure will tend to respond by relaxing to a structure, or set of orientations of the components, which has a lower potential energy in the new stress field than the original structure. The kinetics of the relaxation process depends, of course, on the physical state of the material. Further, a response which involves rearrangement of intermediate range units will be faster in the liquid than the solid. Thus, if the stress is applied to a glass-forming fluid in the transformation range, the response that is effected can be quenched into the glass.

Since the spectral evidence for boroxol rings in  $B_2O_3$  (gl) has also been observed for the melt at temperatures of  $1000^{\circ}C$  and higher (13), it is reasonable to postulate that such a unit is present in  $B_2O_3$  in the transformation region as well. If it is the type of structure suggested, it should respond to stresses applied to the melt, and the stress-induced arrangement should be quenched in the glass. A thin film of vitreous  $B_2O_3$ , prepared by careful expansion of a bubble of the  $B_2O_3$  melt, is formed under stress - the stress is that due to the pressure difference between the inside and outside of the bubble. This stress should induce the planar boroxol rings, if they are present, to become preferentially ordered parallel to the plane of the film.

Although it may be intuitively obvious that this would be the

expected response of a planar unit, it can be seen more clearly by considering a thin-walled spherical shell with a positive internal pressure,  $p_i$ . The shell will exhibit a stress distribution characterized by  $\sigma_r$  and  $\sigma_T$ , the stress components in the radial and tangential directions. It can be shown (14), that  $\sigma_r \approx p_i/2$  and  $\sigma_T = p_i r/2t$ , where  $t$  is the thickness of the shell and  $r$  is the spherical radius. For  $r \gg t$ ,  $\sigma_T \gg \sigma_r$ , so the principal stresses in the spherical film are directed tangentially, i.e. along the surface of the sphere. This situation is analogous to that of a thin film with a force field applied to the film edges directed outward but within the film plane.

Since the material, and specifically its distribution of molecular orientations, is no longer at equilibrium once the force is applied, the effect of such forces will be to rotate molecular units to positions of lower potential energy. If a boroxol ring is a flat unit hooked to neighboring units via three extraannular bonds, application of such outward-directed planar forces should cause the ring to rotate around its center and become closer to parallel to the film plane.

Determination of molecular orientation in polymeric materials has been attempted with a variety of techniques, some of which were reviewed by Wilkes (15). The application of polarized Raman scattering to this problem, particularly in determining orientation of molecular chains in fibers, has received attention as well (16-20). Miller, Exarhos and Risen (16) first employed this technique to demonstrate molecular orientation in a completely amorphous system by showing that  $(PO_3)_n^{11-}$  chains are preferentially oriented with the axis of

$(\text{NaPO}_3)_x$  (gl) fibers drawn from the melt.

The orientational properties of solids manifest themselves in the Raman spectra through the anisotropy of the polarization dependence of Raman-scattered light. Materials whose molecular units are randomly oriented exhibit Raman spectra whose band intensities can be calculated by averaging the polarizabilities over all orientations. These intensities, then, are functions of two quantities (21), the mean value  $\bar{\alpha}$  and the anisotropy,  $\gamma$ , of the derived molecular polarizability elements  $\alpha_{pq}$ , where  $\alpha_{pq} = (\partial^2\alpha/\partial p\partial q)_0$ , and

$$\bar{\alpha} = \frac{1}{3} (\alpha_{xx} + \alpha_{yy} + \alpha_{zz}) \quad (1)$$

$$\gamma^2 = \frac{1}{2} [(\alpha_{xx} - \alpha_{yy})^2 + (\alpha_{yy} - \alpha_{zz})^2 + (\alpha_{zz} - \alpha_{xx})^2 + 6(\alpha_{xy}^2 + \alpha_{yz}^2 + \alpha_{zx}^2)] \quad (2)$$

These two quantities,  $\bar{\alpha}$  and  $\gamma$ , are invariant under any transformation of the macroscopic coordinates of the material. That is, their values, and hence the scattering intensities, are independent of how a bulk sample is oriented in the scattering experiment.

This is not the case if complete or partial molecular ordering occurs in the sample. In such cases at least one unique axis exists. This results in Raman band intensities which depend explicitly on the geometry of the experiment, specifically on the position of the unique axis or axes in reference to the space (laboratory) coordinates of the experiment.

The prominent  $808\text{-cm}^{-1}$  band in the Raman spectrum of  $\text{B}_2\text{O}_3$  (gl) has been shown to be unusual for a glassy system in its uncoupled vibrational character. Assigned to an  $A_1'$  ring-breathing mode of the

boroxol ring, it is strong, relatively sharp, and highly polarized. Thus, it provides an ideal feature for monitoring molecular orientation as a function of film orientation. Any dependence of the  $808\text{-cm}^{-1}$  band's intensity and polarization on spatial orientation of a  $\text{B}_2\text{O}_3$  film different from that of this band in the spectra of bulk samples will indicate that molecular (boroxol) orientation in the film is other than random. Moreover, the boroxol model requires a particular orientation-dependence of the Raman intensities, so comparison of experimental and calculated intensities of the  $\text{A}_1'$  mode of the  $808\text{-cm}^{-1}$  band will provide evidence for or against its occurrence in  $\text{B}_2\text{O}_3$  glass.

Thus, if the boroxol rings exist in vitreous  $\text{B}_2\text{O}_3$  and attain preferential orientation in the film formation process, the intensities and polarization of those Raman bands assigned to boroxol ring vibrations should depend strongly on the orientation of the film in the laboratory coordinate system. Obversely, this dependence supports the existence of orientable flat structures ~ boroxol rings.

In this paper the polarization dependence of the Raman spectra of  $\text{B}_2\text{O}_3(\text{gl})$  films with oriented boroxol rings is calculated as a function of scattering geometry, and the results of the Raman experiments on such films are reported.

Theory

In order to compute the way the intensity of the  $808\text{-cm}^{-1}$  boroxol ring vibration in molecularly oriented films should vary with sample orientation and incident light polarization, it is necessary to consider the derived polarizability in laboratory coordinates. To do that it is useful first to define the coordinate systems.

Geometric Considerations

To specify the results of these experiments completely, three coordinate axes are defined. These are the molecular coordinates  $(x, y, z)$ , the sample (or film) coordinates  $(\bar{x}, \bar{y}, \bar{z})$ , and the space (laboratory) coordinates  $(X, Y, Z)$  of the Raman experiment. The molecular coordinates are those of the boroxol ring with  $z$  taken as the  $C_3$  axis perpendicular to the plane of the ring, so  $x$  and  $y$  lie in this plane. The sample (film) coordinates are defined for the macroscopic shape with  $\bar{z}$  taken as that perpendicular to the plane of the film. The coordinates  $\bar{x}$  and  $\bar{y}$  are equivalent and lie in the plane of the film.

Assuming that the result of the film preparation is that the boroxol rings exist and all are parallel to the plane of the film, there is a unique relationship between the molecular and sample coordinates as shown in Fig. 2. Here  $z$  is parallel to  $\bar{z}$ , and  $x$  and  $y$  vary arbitrarily in the  $\bar{x}\bar{y}$  plane. This relationship, with the  $z$  and  $\bar{z}$  axes being unique, corresponds to Case I of Snyder (20), who calculated polarizabilities for a number of types of partially oriented systems.

The space (laboratory) coordinates are defined by the experimental Raman scattering geometry. As shown in Fig. 3,  $X$  is defined as the direction of propagation of the incident beam, and  $Z$  as that of the

scattered (collected) beam. The directions of polarization (electric field vector  $\vec{E}$ ) of incident and scattered radiation are defined in terms of the spatial coordinates. Commonly light polarized with  $\vec{E}$  in the plane defined by the optical path is taken as V, and that normal to it as H. Thus, polarization in the XZ plane is denoted V and that in direction Y as H.

This notation is sufficient for describing experiments on the amorphous bulk glass. For films, where orientational effects are seen, the sample orientation must be specified as well. An infinite number of film orientations is possible. To specify any one of them in terms of the space (laboratory) coordinates, it is convenient to use the Euler angles and coordinate transformation, which depends on the angles  $\alpha$ ,  $\beta$ , and  $\psi$ . Specification of two of these,  $\theta$  and  $\beta$ , is sufficient to define completely the film's (or molecule's) orientation with respect to the space coordinates, while the third,  $\psi$ , specifies the molecule's angular variation within the film plane and is arbitrary. The coordinates and transformation matrix given by Macaulay (22) were used in these calculations, but the calculations also were done in the two other Euler systems described in references (23) and (24).

Since there are so many possible film orientations, the experiments and calculations were carried out using particular sets of orientations, or "tilts", of which three are shown in Figs. 4a, 4b and 4c. In each of these z is confined to a particular plane defined by the space coordinates as follows. By definition: Tilt 1 is that in which z is confined to the XZ plane ( $\beta = 0^\circ$ ), and  $\theta$  varies from  $0^\circ$  to  $90^\circ$ ; Tilt 2 is that in which z is confined to the XY plane ( $\alpha = 90^\circ$ ),

and  $\beta$  varies from  $0^\circ$  to  $90^\circ$ ; and, Tilt  $\beta$  is that in which  $z$  is confined to the XY plane ( $\beta = 90^\circ$ ), and  $\beta$  varies from  $0^\circ$  to  $90^\circ$ . Thus, a complete specification of the following experiments on a film is given by defining the polarization directions in terms of H and V, and indicating the type and amount of film tilt in terms of  $\alpha$  and  $\beta$ .

#### Derivation of Raman Scattering Intensities

The problem of calculating Raman intensities for the various possible scattering geometries reduces to a determination of the various  $\alpha_{pq}$ , the components of the derived polarizability tensor in the laboratory coordinates, in terms of the derived molecular polarizability elements  $\alpha_{pq}$ . The intensity of Raman scattered light polarized in a particular direction is directly proportional to the square of the relevant  $\alpha_{pq}$ .

For a bulk material with randomly oriented scattering centers, the polarizability components can be obtained by averaging the molecular polarizability components over all orientations of the molecule. The intensity results can then be expressed in terms of the  $\bar{\alpha}$  and  $\gamma$ , given in Eqns 1 and 2. Further, it is known that for that case:

$$\overline{(\alpha_{xx}^2)} = \overline{(\alpha_{yy}^2)} = \overline{(\alpha_{zz}^2)} = \frac{1}{45} [45(\bar{\alpha})^2 + 4\gamma^2] \quad (3)$$

and

$$\overline{(\alpha_{xy}^2)} = \overline{(\alpha_{yz}^2)} = \overline{(\alpha_{zx}^2)} = \frac{1}{15} \gamma^2 \quad (4)$$

for an  $A_1'$  mode of a boroxol ring, of  $D_{3h}$  symmetry,  $\alpha_{pq}$  is given by (25):

$$\underline{\underline{\alpha}}_{pq} = \begin{pmatrix} a & 0 & 0 \\ 0 & a & 0 \\ 0 & 0 & b \end{pmatrix} \quad (5)$$

where  $a = \alpha_{xx} = \alpha_{yy}$ ,  $b = \alpha_{zz}$ , and  $\alpha_{xy}$ ,  $\alpha_{xz}$ , and  $\alpha_{yz}$  are zero. Thus,  $\bar{\gamma}$  and  $\gamma^2$  take the forms  $\bar{\gamma} = (2a + b)/3$  and  $\gamma^2 = (a - b)^2$ . In the limit of  $a \gg b$ , the Raman intensities relative to that for the HH mode were calculated using Eqs 3 and 4 and are given in Table I along with the experimental results for bulk  $B_2O_3$  (g1).

To arrive at intensities for the films which can be compared to the experimental results, appropriate account of the spatial relationships must be taken. The tensor  $\underline{\underline{\alpha}}_{pq}$  is related to  $\underline{\underline{\alpha}}_{PQ}$  by

$$\underline{\underline{\alpha}}_{PQ} = T \underline{\underline{\alpha}}_{pq} T' \quad (6)$$

where  $T$  is the transformation matrix (22) relating the laboratory coordinates  $P, Q$ , to the molecular coordinates,  $p, q$ ; and  $T'$  is its transpose. Using  $\underline{\underline{\alpha}}_{pq}$  given in Eqn 5 with  $T$  yields for Eqn 6:

$$\underline{\underline{\alpha}}_{PQ} = \begin{pmatrix} \alpha_{xx} & \alpha_{xy} & \alpha_{xz} \\ \alpha_{yx} & \alpha_{yy} & \alpha_{yz} \\ \alpha_{zx} & \alpha_{zy} & \alpha_{zz} \end{pmatrix} \quad (7)$$

the square 3 of whose elements are given in Appendix I.

The terms  $\alpha_{yx}$ ,  $\alpha_{zx}$ ,  $\alpha_{yy}$ ,  $\alpha_{zy}$  give rise to the HV, VV, HH, and VH intensities respectively, and are the only components of interest here. Calculated squares of these components for the various film orientations are given in Appendix II, and in Tables II, III and IV the relevant values are given along with the experimental results for the intensities normalized to that of the HH component. All

calculated values assume that the angle of incidence of the light with the film is the same as that with well oriented boroxol rings. This assumption is discussed below.

At most only two of these intensities are predicted to be non-zero for any orientation. The calculated non-zero ratios for the various tilts are, for  $a \gg b$ ; VV/HH for Tilt 1, HV/HH for Tilt 2, and VH/HH for Tilt 3, and are presented in Fig. 5 as a function of the sample tilt angle ( $\theta$  for Tilts 1 and 3,  $\phi$  for Tilt 2).

It is useful to note several of the assumptions that have been made in relating  $\alpha_{pq}$  to  $\alpha_{PQ}$ . One is that the boroxol rings are aligned with the film, so that  $z$  is parallel to  $\bar{z}$ . If this is true of all boroxol rings, the transformation holds for all of them, and, in the absence of other effects, the experimental results would be exactly as predicted by Eqn 7. Similarly if there is preferential but not complete alignment, the experimental results should follow the trends in intensity predicted by Eqn 7.

The other assumption is that the angle of incidence of the light (Raman source) with the film is the same as that with an exactly aligned boroxol ring. Since the refractive index of bulk  $B_2O_3$  (g1) is about 1.43, this holds rigorously only for rings at the surface. Refraction has an effect on some of the measurements at incidence different from 0 or  $90^\circ$ , and on some in which the scattered light is refracted. These effects involve both the identity of the relevant elements in  $\alpha_{PQ}$  and on the optical angles and are discussed later.

ExperimentalGlass Preparation

The  $B_2O_3$  glasses were made by first heating  $H_3BO_3$  (reagent grade) in a Pt crucible at  $1000^{\circ}C$  in an electric furnace for one hour. The melt was then quenched to form a glass according to the following procedures.

Bulk samples of the  $B_2O_3$  glass were made by pouring the melt into a cylindrical stainless steel mold under a stream of dry  $N_2$  at room temperature. Vitreous  $B_2O_3$  films of  $10-20 \mu m$  in thickness were made by first allowing the melt to cool enough to become somewhat viscous. Then a hollow pyrex tube was dipped into the melt to coat one end with molten  $B_2O_3$ . A carefully controlled burst of  $N_2$  was then passed through the tube so as to form a bubble slowly. While the bubble was expanding but nearly full-blown, it was pressed lightly against a stainless steel block so that a flat section of film was obtained. It was possible to obtain reproducible  $B_2O_3$  bubbles with walls nearly as thin as permitted by the surface tension of the melt just above  $T_g$ . For some experiments films as thick as  $50-100 \mu m$  were prepared.

This effort was spent making thin films to assure that the maximum degree of in-plane stress obtainable by surface-tensile-limited film formation was introduced. This was done to obtain the highest practical state of alignment of putative boroxol rings in  $B_2O_3$  (gl).

Sample Handling and Raman Spectra

Because of the hygroscopic nature of  $B_2O_3$  (gl), care was taken to exclude water while handling and measuring the samples. After making some series of measurements in a dry  $N_2$ -flushed sample holder

and some within the spectrometer while the sample itself was flushed with  $N_2$ , the following procedure was found to be sufficient to avoid hydrolysis. The sample was surrounded with  $N_2$  during preparation and transportation to the spectrometer. The films were mounted and studied while under a stream of dry  $N_2$ . Each set of spectra was taken within 15 minutes of sample preparation. After each set of spectra was measured, the  $800-950\text{ cm}^{-1}$  region was measured to detect any scattering at  $880\text{-cm}^{-1}$  due to boric acid formation at the surface, and rejected if any intensity at that frequency was found.

After each sample was mounted, the  $700-900\text{ cm}^{-1}$  region of the Raman spectrum was taken at the four possible combinations of incident and scattering polarization, i.e. HH, HV, VH, VV. These were achieved by appropriate adjustment of the polarization rotator and analyzer. Immediately after taking the spectra in these modes, each was repeated in turn to confirm reproducibility, and the  $880\text{-cm}^{-1}$  region was scanned to confirm the absence of Raman-detectable hydrolysis.

To obtain a spectrum of the bulk glass, the cylindrical sample was cleaved in half and positioned as shown in Fig. 6a with the laser beam impinging on the top surface about 1 mm from the cloven edge, and radiation scattered at  $90^\circ$  was collected from this face.

Raman spectra of the  $B_2O_3$  (gl) films were obtained by mounting them at the appropriate orientations and collecting the light scattered at  $90^\circ$  to the incident beam. Due to the thinness of the films, there were different sample mounting requirements and problems for each orientation. The spectra at Tilt 1 ( $\phi = 0^\circ$ ) were obtained using

the sample mount shown in Fig. 6b. The vitreous film was mounted over a hole drilled through a blackened metal plate. The use of the plate allowed for more accurate control of  $\theta$ . Spectra were taken for  $\theta = 0, 30, 45, 60$ , and  $90^\circ$ . The spectra in Tilts 2 and 3 were obtained by tilting the film in the beam to the desired alignment. Since the mounting arrangement used in Tilt 1 measurements was not applicable to these orientations, these angles could be measured only with lower accuracy. At least three determinations were made for each angle for these cases, at the angles of  $\phi \approx 0, 45$ , and  $90^\circ$  for Tilt 2 ( $\theta = 90^\circ$ ), and  $\phi = 0, 45$ , and  $90^\circ$  for Tilt 3 ( $\phi = 90^\circ$ ), but the uncertainty in the average angular values could be as high as  $5^\circ$ .

As appropriate, samples were partially masked to eliminate extraneous scattering from the edges of the film, as shown in Fig. 3. In some measurements of Tilt 2, thicker films (50-100  $\mu\text{m}$ ) were used, since for  $\theta = 90^\circ$  and  $0 < \phi < 90^\circ$  it is difficult to get the source into the edge of a 10-20  $\mu\text{m}$  film without reflecting some of the light from the face. With 50  $\mu\text{m}$  films the focused laser beam passes through the edge of the film.

Raman spectra of the vitreous  $\text{B}_2\text{O}_3$  samples were taken on a Jarrell-Ash 25-300 laser Raman spectrometer using the 514.5 nm line for excitation. The spectral resolution was ca.  $5 \text{ cm}^{-1}$  and the laser power employed was ca. 750  $\text{mW}$ . The optical arrangement in the vicinity of the sample is shown in Fig. 3. Scattered light was optically scrambled after polarization analysis and before passing the entrance slit of the monochromator. Depolarization ratios of the standard  $\text{CCl}_4$  were adequately reproduced with this spectrometer.

### Results

The observed intensities of the  $808\text{-cm}^{-1}$  Raman band of bulk vitreous  $\text{B}_2\text{O}_3$  for the various polarization combinations are given relative to the intensity of the HH component in Table I. The observed intensities of this band for film samples for Tilts 1, 2 and 3, again relative to the strongest band observed in each film orientation, the HH polarization component, are given in Tables II, III, and IV, respectively.

The results obtained on the bulk samples are in good agreement with those calculated for complete disorder. The values for the HV, VH and VV components relative to HH are calculated to be 0.13, in the limit  $a \gg b$  (i.e. with  $b$  ( $\alpha_{zz}$ ) set to zero), and they are observed to be  $0.15 \pm 0.03$ ,  $0.16 \pm 0.03$ , and  $0.11 \pm 0.03$ . These values, averaging  $0.14 \pm 0.03$ , are a bit higher than the other reported value of 0.07 (13), which presumably also has an experimental error of about  $\pm 0.03$ . Together, these values confirm that the mode is highly polarized, and that if its  $\tilde{\alpha}$  and  $\gamma^2$  have the form given above for a boroxol ring,  $b$  is in the range  $0 \leq b \leq 0.15a$ , or  $a \gg b$ .

The results for the polarization ratios for the  $\text{B}_2\text{O}_3(\text{gl})$  films demonstrate two main points. First, the units which vibrate at  $808\text{-cm}^{-1}$  are not randomly arrayed; they are ordered to a significant degree. Second, the ordering of these units is approximately as calculated for boroxol rings; that is, flat molecular units parallel to the surface of the film. Although these conclusions will be qualified in detail, by noting that preferential ordering does not require that all boroxol rings be exactly parallel to the surface, as the calculations have assumed, noting some optical effects not

considered so far, and comparing the detailed data with the calculated results, the data are essentially those predicted for oriented boroxol rings.

The comparisons of calculated and experimental results that lead to the main conclusions are these. The film data are very different from those for bulk  $B_2O_3$  (gl). For the bulk  $B_2O_3$  (gl), all components other than HH have relative intensities of only  $0.14 \pm 0.03$ . However, as shown in Tables II, III, and IV, for the films one component other than HH becomes quite strong as the angle is varied. Moreover, the one which does become strong, VV in Tilt 1, HV in Tilt 2, and VH in Tilt 3, is the one calculated to gain intensity upon changing film orientation in the prescribed manner. In addition, with two exceptions, all of those relative intensities calculated to be zero in this idealization are  $0.15 \pm 0.06$ . These values may be taken to be effectively zero for the purpose of comparing calculated and observed ratios. Their difference from zero results partly from the fact that not all of the units are perfectly oriented, even though the degree of orientation is high, and from some optical effects discussed below.

The two relative intensities which should also be small, but are not, are: first, those for which the HH component derives exclusively from the polarizability element  $b$ ,  $\phi = 90^\circ$  in Tilt 2 and  $\phi = 90^\circ$  in Tilt 3, and second the VH/HH ratio at  $\phi = 45^\circ$  in Tilt 2. For the former ones, where HH is given by  $b^2$ , it is important to note that since  $a \gg b$ , the HH component is very weak and all of

the other components are even weaker. Taking  $b \approx 0.05a$  as a reasonable estimate from the bulk data, the HH band for these orientations is expected to be only  $2.5 \times 10^{-3}$  as intense as it is at the other extreme angle in each relevant Tilt. This means that the ratios at issue are, relatively, 0/0.0025, and experimental noise is a significant factor since each of them is the result of dividing two very weak bands. As discussed below, the observed values can be accounted for completely in a more straightforward way. If there is an alignment error of about  $3^\circ$ , the expected values for the ratios are not zero, but about 0.8. Alignment errors of  $1-4^\circ$  are sufficient to account for all of these observations and are reasonable estimates of the experimental uncertainty. More relevant than the errors that show up as a result of the HH elements becoming small in those cases is the very fact that they do become very small, since these HH components are calculated to arise only from the element  $b^2$ , which is small.

While inspection of Tables II, III, and IV shows that the types of effects predicted by the model are observed, this may be clearer from the plots of the calculated and observed data in Fig. 7. There it is seen that the VV/HH ratios go through a maximum as  $\theta$  is varied, while the VH/HH and HV/HH ratios do not vary.

DISCUSSION

The premise of this work was the following. If boroxol rings exist and have their postulated properties, then they should orient preferentially in a film formed under tensile stress. And, if they do exist with these properties and orient, the polarization dependence of a band in the Raman spectrum due to the ring-unit should have a predictable film-orientation dependence. For the ideal case in which all boroxol rings are oriented parallel to the film's surface, the predicted dependence, detailed above and in the accompanying tables and appendices, is that in each "tilt" two of the intensity ratios should be non-zero at some varied angle, while the other ratios should be zero at all angles. The two non-zero ratios are HH/HH and VV/HH in Tilt 1, HH/HH and HV/HH in Tilt 2, and HH/HH and VH/HH in Tilt 3. Experimental observations of this sort clearly would be consistent with the presence of boroxol rings. What such findings would prove, though, is that a unit with a vibrational mode at the frequency of observation ( $808\text{-cm}^{-1}$ ) exists and is orientable by the application of a tensile stress, that it has at least one unique symmetry axis along which the polarizability element is different from that along the other two principal axes, and that the scattering of greatest intensity results from polarizability along the other two principal axes, which are preferentially parallel to the surface of the film.

The main experimental finding in this study is that the predicted pattern of intensity ratios is observed. This is clearest in the data for Tilts 1 and 3. However, the complete analysis of the results and the experiments themselves requires some

rather involved considerations, which take into account optical effects, the reality of less-than-ideal orientation, and experimental error.

There are several sources of experimental error, including noise and uncertainties in orientation. As mentioned earlier, noise may be important in those cases ( $\phi = 90^\circ$  in Tilt 2,  $\psi = 90^\circ$  in Tilt 3) where the ratio of two extremely weak bands is calculated. Uncertainties in film orientation result partly from the difficulty in precisely aligning and handling ca  $20\mu$ -thick films of hygroscopic material, and partly from the lack of perfect flatness of the films. While considerable care was taken and the spectra were reproduced a number of times, the angles are known imprecisely. This has several ramifications, but the most important is that the zero-valued intensity ratios can take non-zero values - up to 0.06 in cases where HH is strong, and much higher where the HH intensity is ideally proportional to  $b^2$ . For example in Tilt 1 if  $\theta = 90^\circ$  and  $\phi = 10^\circ$  instead of  $\psi = 90^\circ$  and  $\phi = 0^\circ$ , the ratio HV/HH becomes 0.03 instead of zero and is somewhat closer to the observed value of  $0.13 \pm 0.05$ . The net effect of several small angular errors plus some scattering from unaligned units explains the fact that many of the ratios calculated to be zero are, in fact, observed to be on the order of 0.1. In those special cases noted above ( $\phi = 90^\circ$  in Tilt 2, and  $\psi = 90^\circ$  in Tilt 3) where ideally zero valued ratios are quite large, angular uncertainty is particularly important. In them, changing the angles by only  $1-4^\circ$  takes the zero valued ratios to the 0.56-0.98 observed, so it is not unreasonable to ignore their

difference from zero in comparing the observed data to those computed for the ideal case.

There are several optical effects of potential significance in these experiments. At incident angles other than normal to the entrance surface, refraction occurs. This changes the angle of incidence between the light and sub-surface units and, in the process, its direction of incident light polarization. These effects are discussed in Appendix III, in which an approximation to the effect of changing the incident angle is treated. The effect of changing the direction of light polarization is to change the form of the polarizability tensor because the  $\vec{E}$  vector projection on the molecular coordinate system is changed. However, derivation of the new tensor shows that the new terms are nearly offsetting in their effect on the intensity ratios. Another effect is that certain scattered light rays in certain orientations attempt to exit at the critical angle,  $\theta_c$ , relative to the surface. As they cannot, they are "light piped". While this can affect absolute intensities, it does not have a significant impact on any of the intensity ratios. Finally, polarization-selective reflection, especially near Brewster's angle, can be important in this sort of experiment. There is one case where it may be significant here; VV/HH at  $\beta = 30^\circ$  in Tilt 1, in which the HH intensity may be made lower while the VV is unaffected. This may explain why VV/HH is higher for  $\beta = 30^\circ$  than for  $\beta = 60^\circ$  in Tilt 1. Overall, the optical effects considered here do not invalidate the conclusion that the calculated trends are observed.

Finally, the degree of molecular orientation in the film samples

may be considered. In light of the sources of error and the complexity of the analysis and phenomena, it is not feasible to compute the degree of order with certainty. The best estimate can be made by using the measurements at Tilt 3,  $\theta = 45^\circ$ , VH/HH, and Tilt 2,  $\phi = 45^\circ$ , HV/HH, since both components of each ratio are reasonably strong bands. For each ratio,  $I_{ij}/I_{HH}$ , both  $I_{ij}$  and  $I_{HH}$  are sums of contributions from the  $N_1$  oriented and the  $N_2$  random population oscillators. The forms of the contributions to the total intensity in each orientation from ordered units and from a random population of oscillators are known. From them and the ratios a quite high degree of orientation is found for those units responsible for the scattering. Given this and the fact that the refractive effects do not appear to be overriding, it is reasonable to suppose that many of these centers are near the surface.

Conclusion

The orientation dependence of the polarization dependence of the Raman spectral band at  $808\text{-cm}^{-1}$  of thin  $\text{B}_2\text{O}_3(\text{gl})$  films, formed under tensile stress, is consistent with the existence of oriented boroxol rings. Since this band also appears in the spectra of  $\text{B}_2\text{O}_3$  melts and bulk glasses, these data support the conclusion that boroxol rings exist in  $\text{B}_2\text{O}_3(\text{gl})$ .

Acknowledgments

This work was supported in part by the Office of Naval Research. The support and use of facilities of the Materials Research Laboratory of Brown University, sponsored by the National Science Foundation, is gratefully acknowledged. The authors thank the Montedison Group for the award of a Montedison Fellowship in Chemistry to C.F.W. It also is a pleasure to acknowledge helpful discussions with Professor P.J. Bray and his students, and Dr. J. Mikkelsen and Dr. F. Galeener.

References

1. J. Goubeau and H. Keller, *Z. Anorg. allg. chem.* 272, 303 (1953).
2. J. Krogh-Moe, *Ark, Kemi* 12, 475 (1958).
3. L.A. Kristiansen and J. Krogh-Moe, *Physics Chem. Glasses* 9(3), 96 (1968).
4. J. Krogh-Moe, *J. Non-Cryst. Solids* 1, 269 (1969).
5. R.L. Mozzi and B.E. Warren, *J. Appl. Crystallogr.* 3, 251 (1970).
6. W.L. Konijnendijk and J. M. Stevels, *J. Non-Cryst. Solids* 18, 307 (1975).
7. T.W. Bril, *Philips, Res. Repts. Suppl. No. 2* (1976).
8. J.P. Bronswijk and E. Strijks, *J. Non-Cryst. Solids* 24, 145 (1977).
9. G.E. Jellison, Jr., L.W. Panek, P.J. Bray, and G. B. Rouse, Jr., *J. Chem. Phys.* 66, 802 (1977).
10. F.L. Galeener, G. Lucovsky and J.C. Mikkelsen, Jr., *Physical Review B* 22, 3983 (1980).
11. C.F. Windisch and W.M. Risen, Jr., to be published.
12. S.R. Elliot, *Philos. Mag.* B37, 435 (1978).
13. G.E. Walrafen, S.R. Samanta and P.N. Krishnan, *J. Chem. Phys.* 72, 113 (1980).
14. N.P. Suh, A.P.L. Turner, *Elements of the Mechanical Behavior of Solids*, McGraw-Hill Book Co., New York, 1975, p 74.
15. T.L. Wilkes, *Adv. Polymer Sci.* 8, 91 (1971).
16. P.J. Miller, G.J. Exarhos and W.M. Risen, Jr., *J. Chem. Phys.* 59, 2796 (1973).
17. P.W. Higgs, *Proc. R. Soc. A220*, 472 (1953).
18. S.W. Corneli and J.L. Koenig, *J. Appl. Phys.* 39, 4883 (1968).
19. D. I. Bower, *J. Polym. Sci B* 10, 2135 (1972).

20. R.G. Snyder, J. Mol. Spec. 37, 353 (1971).
21. E.B. Wilson, Jr., J.C. Decius and Paul C. Cross, Molecular Vibrations, McGraw-Hill Book Company, Inc., New York, 1955.
22. W. H. Macaulay, Solid Geometry, Cambridge University Press, London, 1930, pp 60-62.
23. G. Arfken, Mathematical Methods for Physicists, Academic Press, New York, 1970, pp 178-180.
24. P. Frost, Solid Geometry, MacMillan & Co., London, 1875, p 100.
25. R. Loudon, Adv. Phys. 8, 423 (1964).
26. T. F. Soules and A. K. Varshneya, J. Am. Ceram. Soc. 64, 145 (1981).

TABLE I

Calculated and Observed Raman Intensities of the  $808 \text{ cm}^{-1}$  Band of Bulk  $\text{B}_2\text{O}_3$  (g1) for the Various Scattering Configurations Relative to the Intensity of the Band for the HH Configuration

	HH	HV	VH	VV
Calc.	1.0	0.13	0.13	0.13
Obs.	1.0	$0.15 \pm 0.03$	$0.16 \pm 0.03$	$0.11 \pm 0.03$

TABLE II  
Calculated and Observed Raman Intensity Ratios for  $B_2O_3$  (gl) Films  
in Tilt 1 ( $\phi = 0^\circ$ )

$\alpha$	HH	HV	VH	VV
element <sup>(1)</sup>	$a^2$	0	0	0
$90^\circ$ calc ratio <sup>(2)</sup>	1.0	0	0	0
obs. ratio	1.0	$0.13 \pm .05$	$0.13 \pm .05$	$0.16 \pm .07$
element	$a^2$	0	0	$3(a-b)^2/16$
$60^\circ$ calc ratio	1.0	0	0	$3(a-b)^2/16a^2$
obs. ratio	1.0	$0.13 \pm .05$	$0.15 \pm .06$	$.33 \pm .06$ <sup>(3)</sup>
element	$a^2$	0	0	$(a-b)^2/4$
$45^\circ$ calc ratio	1.0	0	0	$(a-b)^2/4a^2$
obs. ratio	1.0	$0.15 \pm .03$	$0.16 \pm .03$	$0.56 \pm .06$ <sup>(3)</sup>
element	$a^2$	0	0	$3(a-b)^2/16$
$30^\circ$ calc ratio	1.0	0	0	$3(a-b)^2/16a^2$
obs. ratio	1.0	$0.14 \pm .05$	$0.16 \pm .05$	$.44 \pm .06$ <sup>(3)</sup>
element	$a^2$	0	0	0
$0^\circ$ calc ratio	1.0	0	0	0
obs. ratio	1.0	$0.11 \pm .03$	$0.13 \pm .03$	$0.2 \pm .07$

(1) Element means the relevant element in the  $\alpha_{PQ}^2$  tensor (Appendix I)

(2) All calculated values are based on the assumption that the angle of incidence of the light with the film is the same as that with completely aligned boroxol rings (see text). The ratios are with respect to the HH intensity.

(3) Although measured values fell in a narrower range than specified in these cases, these limits were assigned after consideration of the observed ranges in all cases.

TABLE III

Calculated and Observed Raman Intensity Ratios for  $B_2O_3$  (g) Films  
in Tilt 2 ( $\theta = 90^\circ$ )

	HH	HV	VH	VV
element <sup>(1)</sup>	$a^2$	0	0	0
$0^\circ$ calc ratio <sup>(2)</sup>	1.0	0	0	0
obs. ratio	1.0	$0.13 \pm .05$	$0.13 \pm .05$	$0.16 \pm .07$
element	$(3a+b)^2/16$	$3(a-b)^2/16$	0	0
$30^\circ$ calc ratio	1.0	$3(a-b)^2/(3a+b)^2$	0	0
element	$(a+b)^2/4$	$(a-b)^2/4$	0	0
$45^\circ$ calc ratio	1.0	$(a-b)^2/(a+b)^2$	0	0
obs. ratio	1.0	$0.81 \pm 0.14$	$0.61 \pm .14$	$0.2 \pm 0.1$
element	$(a+3b)^2/16$	$3(a-b)^2/16$	0	0
$60^\circ$ calc ratio	1.0	$2(a-b)^2/(a+3b)^2$	0	0
element	$b^2$	0	0	0
$90^\circ$ calc ratio	1.0	0	0	0
obs. ratio	1.0	$0.56 \pm ^*(3)$	$0.96 \pm ^*(3)$	$0.68 \pm ^*(3)$

(1) See footnote (1), Table II

(2) See footnote (2), Table II

(3) See text

TABLE IV

 Calculated and Observed Raman Intensity Ratios for  $B_2O_3$  (gl) Film  
 in Tilt 3 ( $\phi = 90^\circ$ )

$\phi$		HH	HV	VH	VV
$0^\circ$	element <sup>(1)</sup>	$a^2$	0	0	0
	calc ratio <sup>(2)</sup>	1.0	0	0	0
	obs. ratio	1.0	$0.11 \pm .03$	$0.13 \pm .03$	$0.2 \pm .08$
$30^\circ$	element	$(3a+b)^2/16$	0	$3(a-b)^2/16$	0
	calc ratio	1.0	0	$3(a-b)^2/(3a+b)^2$	0
	obs. ratio	$(a+b)^2/4$	0	$(a-b)^2/4$	0
$45^\circ$	calc ratio	1.0	0	$(a-b)^2/(a+b)^2$	0
	obs. ratio	1.0	$0.15 \pm .08$	$0.79 \pm 0.10$	$0.18 \pm .05$
	element	$(a+3b)^2/16$	0	$3(a-b)^2/16$	0
$60^\circ$	calc ratio	1.0	0	$3(a-b)^2/(a+3b)^2$	0
	element	$b^2$	0	0	0
	calc ratio	1.0	0	0	0
$90^\circ$	obs. ratio	1.0	$0.56 \pm \star^{(3)}$	$0.96 \pm \star^{(3)}$	$0.68 \pm \star^{(3)}$

(1) See footnote (1), Table II

(2) See footnote (2), Table II

(3) See text.

## Appendix I

Squares of the Elements of the Polarizability Tensor  $\alpha_{PQ}$  in Terms  
of the Molecular Coordinates

The polarizability tensor in laboratory coordinates is  $\alpha_{PQ}$ , and the squares of its elements, which are proportional to the experimental Raman intensities, are elements of the tensor  $\alpha_{PQ}^2$ , where:

$$\alpha_{PQ}^2 = \begin{pmatrix} i & j & k \\ l & m & n \\ o & p & q \end{pmatrix}$$

and,

$$i = [a(\sin^2\phi + \cos^2\phi \cos^2\theta) + b \cos^2\phi \sin^2\theta]^2$$

$$m = [a(\cos^2\phi + \sin^2\phi \cos^2\theta) + b \sin^2\phi \sin^2\theta]^2$$

$$q = (a \sin^2\theta + b \cos^2\theta)^2$$

$$j = l = (a-b)^2 \sin^2\phi \cos^2\phi \sin^2\theta$$

$$k = o = (a-b)^2 \cos^2\phi \sin^2\theta \cos^2\theta$$

$$n = p = (a-b)^2 \sin^2\phi \sin^2\theta \cos^2\theta$$

## Appendix II

The Polarizability Tensors for the Three Experimental Film Sample Orientations

The experimental Raman intensities are proportional to the squares of the elements of the tensor  $\underline{\alpha}_{PQ}$ . As given in Appendix I, these squares are elements of the tensor  $\underline{\alpha}_{PQ}^2$ , where

$$\underline{\alpha}_{PQ}^2 = \begin{pmatrix} i & j & k \\ l & m & n \\ o & p & q \end{pmatrix}$$

For the three experimental arrangements, or Tilts, studied in this work, the elements of  $\underline{\alpha}_{PQ}^2$  are:

Tilt 1 ( $\epsilon = 0^\circ$ )

$$i = (a \cos^2 \epsilon + b \sin^2 \epsilon)^2$$

$$m = a^2$$

$$j = (a \sin^2 \epsilon + b \cos^2 \epsilon)^2$$

$$k = o = (a^2 + b^2) \sin^2 \epsilon \cos^2 \epsilon$$

$$l = 1 = n = p = 0$$

$$n = 1 = l = 1 = n = p = 0$$

$$i = (a \sin^2 \phi + b \cos^2 \phi)^2$$

$$m = (a \cos^2 \phi + b \sin^2 \phi)^2$$

$$q = b^2$$

$$j = 1 = (a-b)^2 \sin^2 \phi \cos^2 \phi$$

$$k = o = n = p = 0$$

## Appendix II - page 2

Tilt 3 ( $\phi = 90^\circ$ )

$$i = a^2$$

$$m = (a \cos^2 \theta + b \sin^2 \theta)^2$$

$$q = (a \sin^2 \theta + b \cos^2 \theta)^2$$

$$n = p = (a-b)^2 \sin^2 \theta \cos^2 \theta$$

$$j = l = o = k = 0$$

## APPENDIX III

It is possible to describe the optical effects in these experiments more completely by including internal reflections, polarization-selective reflection, and refraction. Although each can contribute, and certain of the "light-piping" effects may be significant in determining absolute intensities in certain orientations, the most important effect to consider is refraction. Refraction of the incident ray makes the angle of incidence of the light relative to aligned scattering centers different from that relative to the entrance surface. This alters the functional dependence of the experimental scattered intensities on the various polarizability components.

From an analysis of this functional dependence, it is clear that a reasonable approximation to the overall refraction effect is to consider only the change in incident angle with respect to the scattering centers. That is because the effects of changing the functional forms of the polarizability tensor elements nearly offset one another. A simple calculation can be done within this approximation if it is assumed that the experimental scattering geometry, the angle between the refracted incident and scattered light, remains at  $90^\circ$ , and that refraction does not materially affect the collected fraction of scattered light. This is equivalent to the case of a rotated film with no refraction.

The "new" tilt angle, that incident on a scattering center within the sample, can be calculated using Snell's law and the bulk refractive index of  $B_2O_3$  glass,  $n = 1.48$ . The effect of these changes on the calculated relative intensities ( $a \gg b$ ) is

shown below for Tilt 1. Here, calc' refers to values calculated by including refraction-caused changes in the tilt angle, and calc refers to the relative intensities at nominal experimental angles.

Tilt 1	Nominal $\theta$	HH/HH	HV/HH	VH/HH	VV/HH
calc	90	1.0	0	0	0
<u>calc'</u>		1.0	0	0	0
calc	60	1.0	0	0	0.19
<u>calc'</u>		1.0	0	0	0.10
calc	45	1.0	0	0	0.25
<u>calc'</u>		1.0	0	0	0.18
calc	30	1.0	0	0	0.19
<u>calc'</u>		1.0	0	0	0.23
calc	0	1.0	0	0	0
calc'		1.0	0	0	0

As can be seen, the refraction-effects are predicted to be significant, but they alter only the relative intensity values of the non-zero components shown (VV/HH). The zero-valued components remain zero. Thus, conclusions based on the observation of the trends (e.g. the dependence on VV/HH only in Tilt 1) are not affected by this aspect of refraction. Moreover, the predicted effect of refraction was not observed in these experiments; rather the data followed the more idealized calculations. This may mean that most of the scattering centers involved in these measurements were at or near the surface.

Figure Captions

Figure 1. Representation of the boroxol ( $B_2O_3$  ring structure. The three extra-annular oxygens are bound to trigonal planar B atoms and are the only atoms bound to the ring. The dotted lines from these oxygens to the rest of the network are drawn to emphasize that the extra-annular dihedral angles and those angles with vertices at those oxygens are not defined by the model.

Figure 2. Definitions of the three-coordinate systems, as noted on the figure.

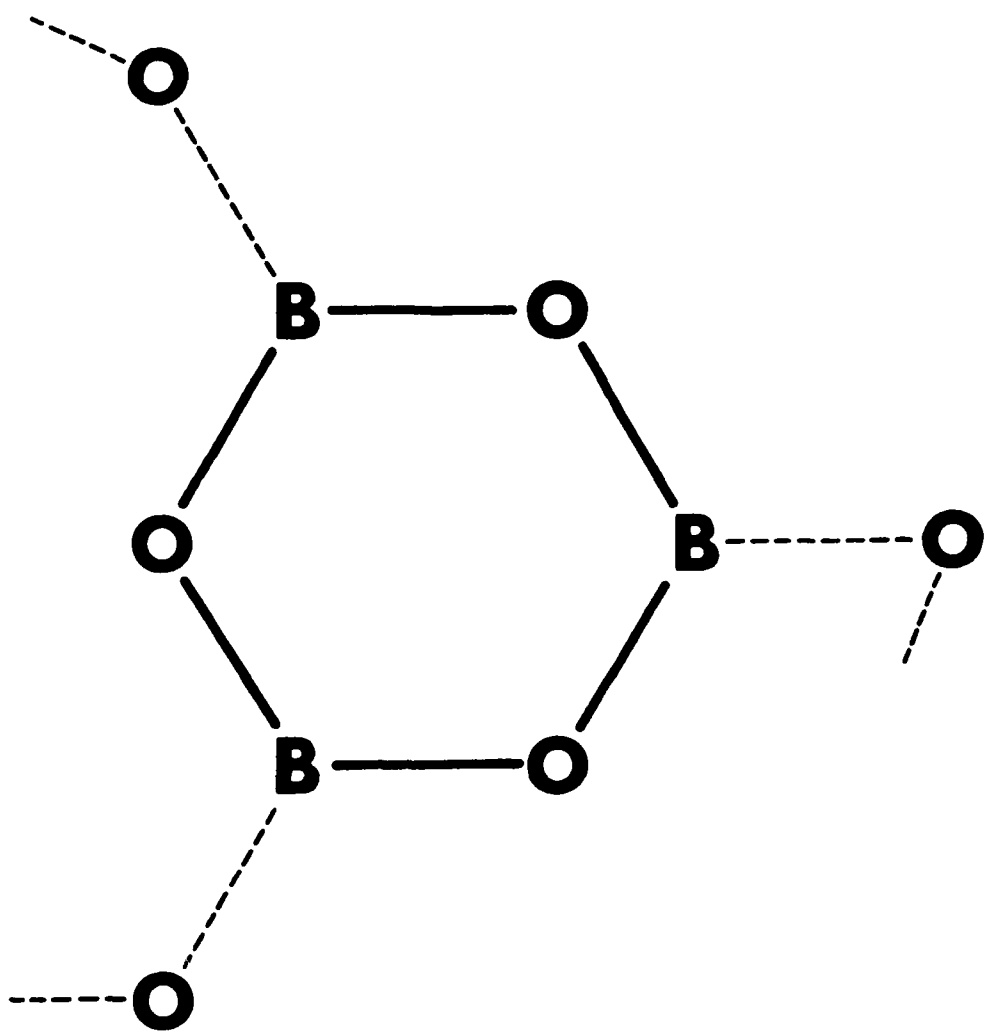
Figure 3. Experimental arrangement for Raman scattering. Two film orientations are shown: (a) Tilt 1,  $\theta = 45^\circ$ ; (b) Tilt 2,  $\phi = 90^\circ$ . Figure (b) also corresponds to Tilt 3,  $\theta = 90^\circ$ .

Figure 4. Definitions and representations of the orientations of  $B_2O_3$  films in the three "Tilts". In Tilt 1 (a)  $\theta$  varies in the ZX plane; in Tilt 2 (b)  $\phi$  varies in the XY plane; and, in Tilt 3 (c)  $\theta$  varies in the ZY plane.

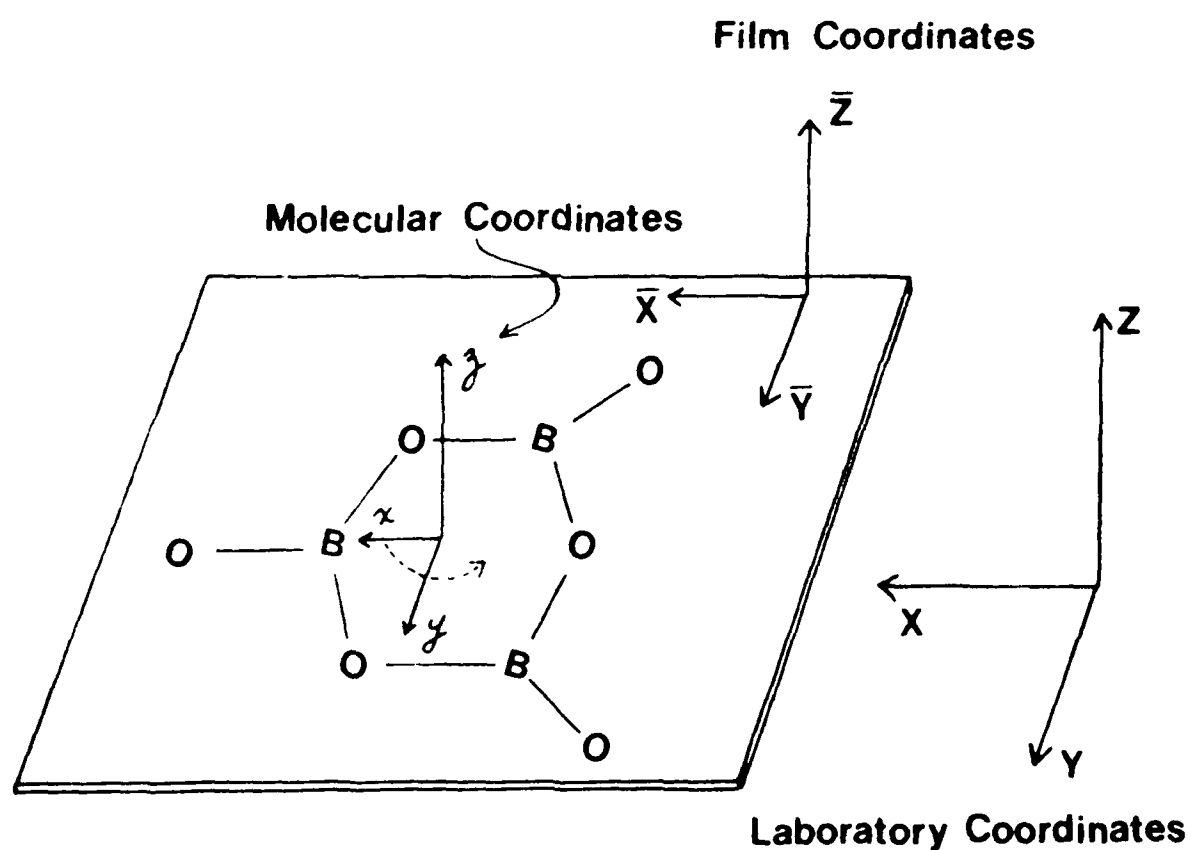
Figure 5. Plots of the calculated intensity in the non-zero orientation relative to that in the HH orientation,  $i/HH$ , versus tilt angle for the case  $a \gg b$ . Plot (a) is for Tilt 1, tilt angle is  $\theta$ , and  $i/HH$  is VV/HH. Plot (b) applies to Tilt 2, tilt angle  $\phi$ , and Tilt 3, tilt angle  $\theta$ , and represents HV/HH in Tilt 2 and VH in Tilt 3.

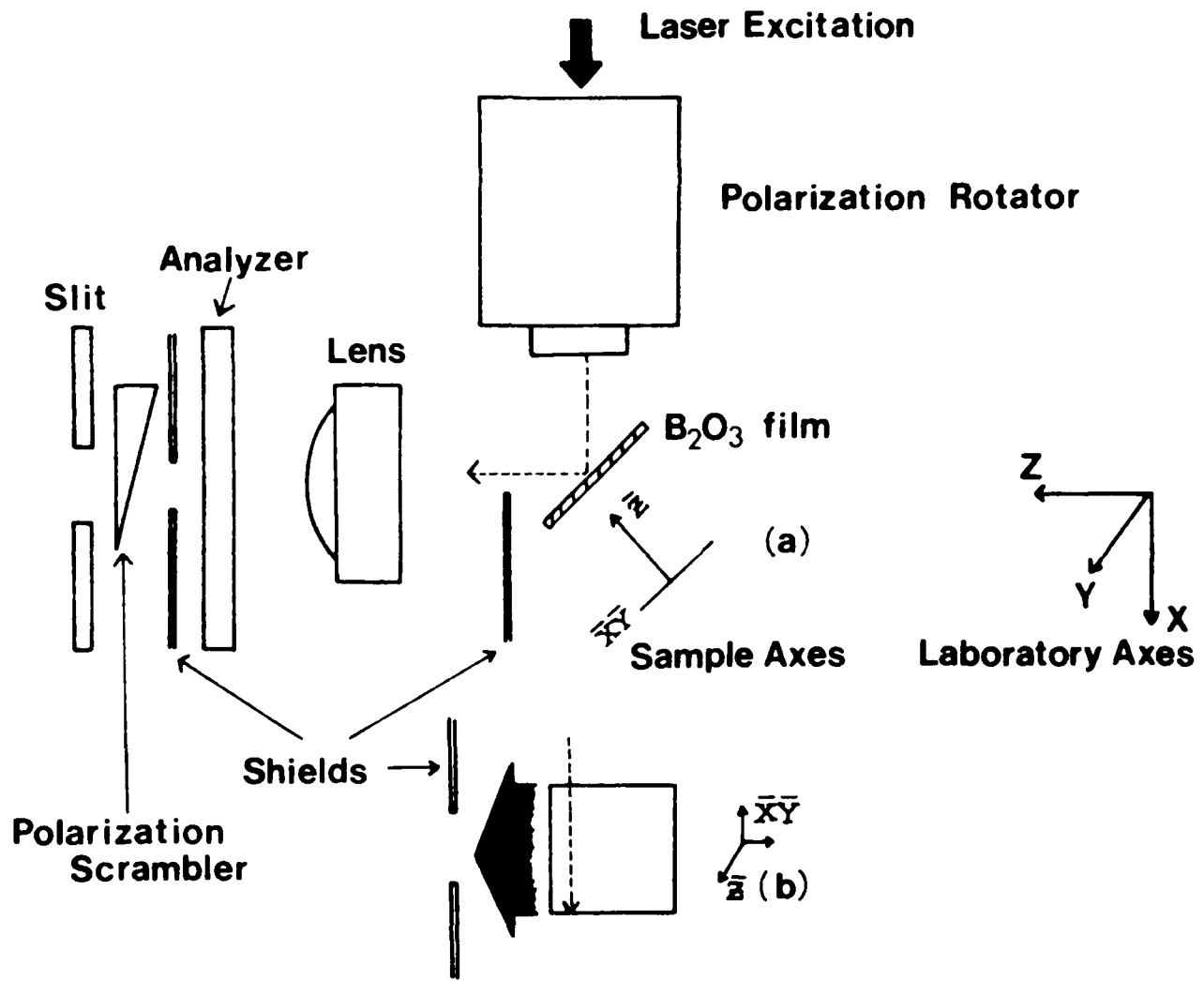
Figure 6. Sample geometry and the directions of the incident and scattered (collected) light in laboratory coordinates. Here, (a) is the bulk (cloven block) sample, and (b) shown the sample mounting used for Tilt 1,  $0 < \theta < 90^\circ$ .

Figure 7. Comparison of the calculated and observed dependence of relative intensity on tilt angle ( $\theta$ ) for Tilt 1. The upper graph refers to the VV/HH ratio, while the lower one applies to the HV/HH and VH/HH ratios.

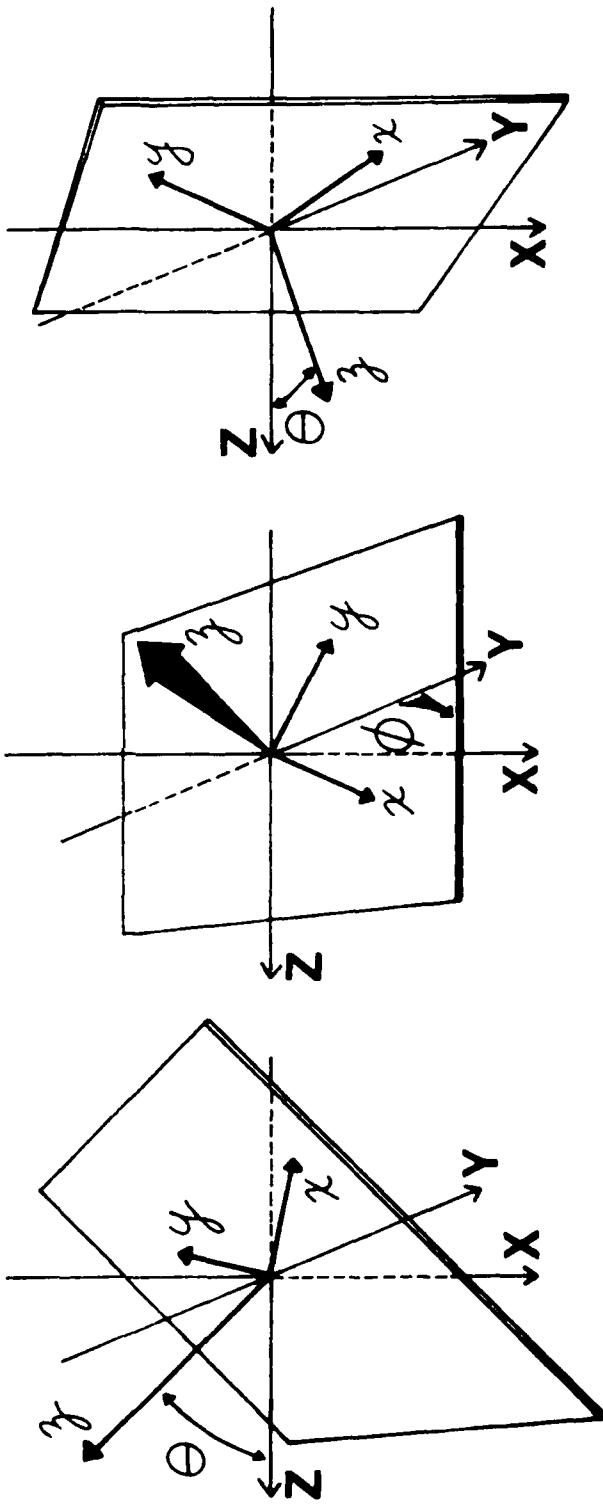


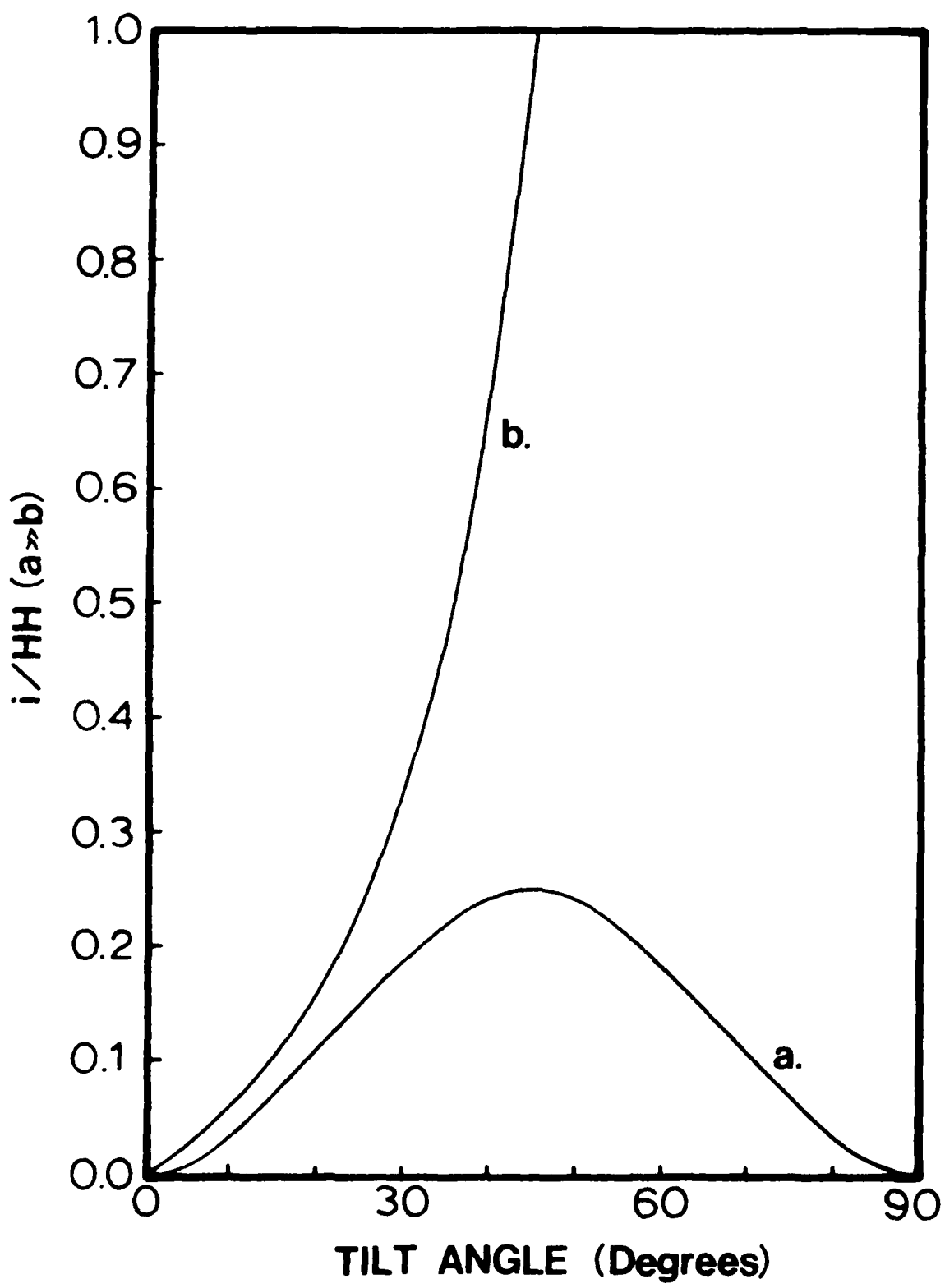
## COORDINATE DEFINITIONS



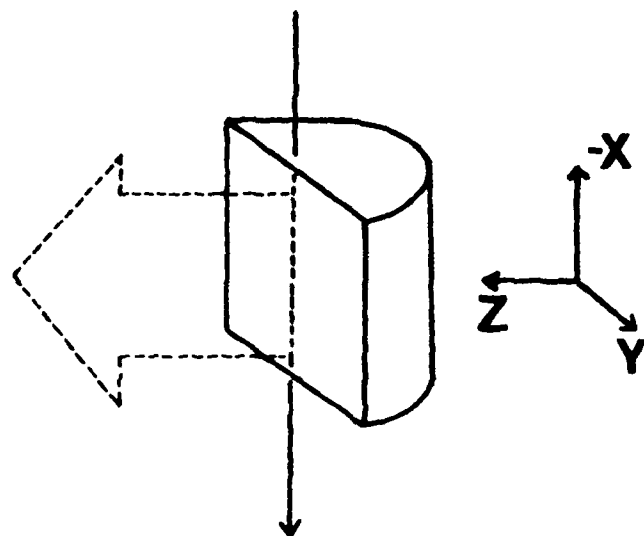


a. TILT 1      b. TILT 2      c. TILT 3

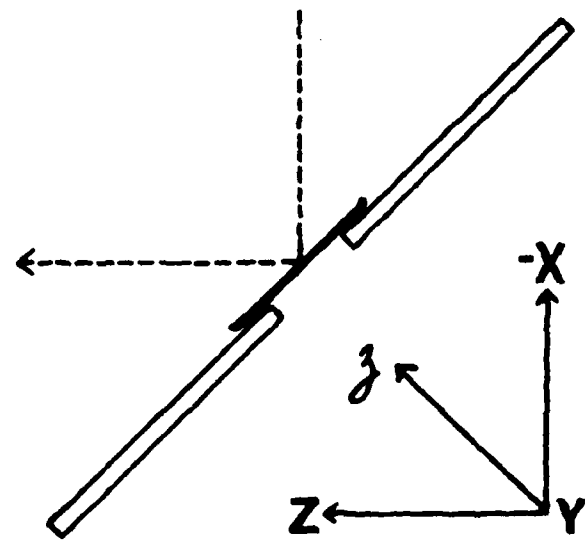


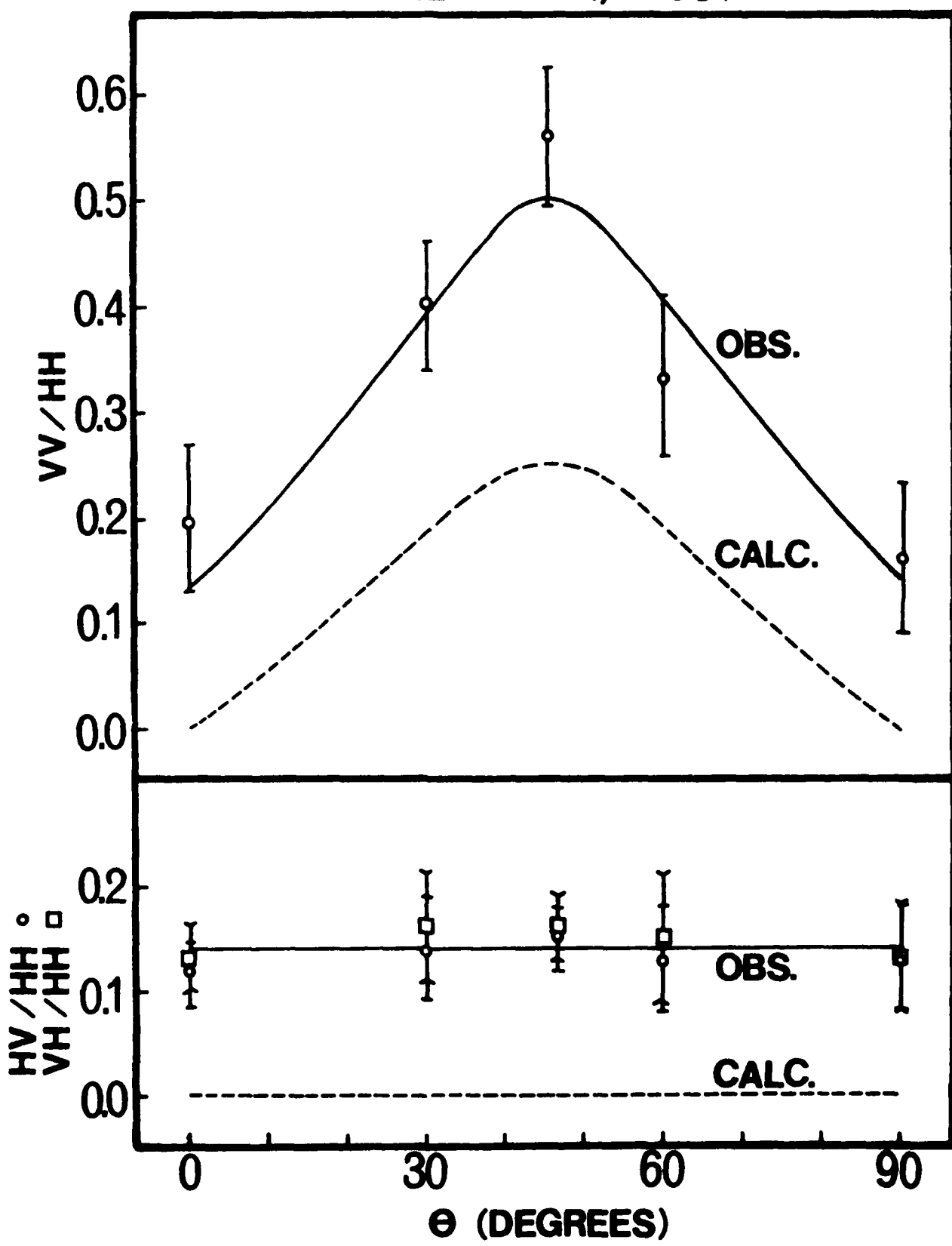


a.



b.



TILT 1 ( $\phi = 90^\circ$ )

TECHNICAL REPORT DISTRIBUTION LIST, 356A

<u>No.</u> <u>Copies</u>	<u>No.</u> <u>Copies</u>		
Dr. Stephen H. Carr Department of Materials Science Northwestern University Evanston, Illinois 60201	1	Picatinny Arsenal Attn: A. M. Anzalone, Building 3401 SMUPA-FR-M-D Dover, New Jersey 07801	1
Dr. M. Broadhurst Bulk Properties Section National Bureau of Standards U.S. Department of Commerce Washington, D.C. 20234	2	Dr. J. K. Gillham Department of Chemistry Princeton University Princeton, New Jersey 08540	1
Professor G. Whitesides Department of Chemistry Massachusetts Institute of Technology Cambridge, Massachusetts 02139	1	Dr. E. Baer Department of Macromolecular Science Case Western Reserve University Cleveland, Ohio 44106	1
Dr. D. R. Uhlmann Department of Metallurgy and Material Science Massachusetts Institute of Technology Cambridge, Massachusetts 02139	1	Dr. K. D. Pae Department of Mechanics and Materials Science Rutgers University New Brunswick, New Jersey 08903	1
Naval Surface Weapons Center Attn: Dr. J. M. Augl, Dr. B. Hartman White Oak Silver Spring, Maryland 20910	1	NASA-Lewis Research Center Attn: Dr. T. T. Serofini, MS-49-1 21000 Brookpark Road Cleveland, Ohio 44135	1
Dr. G. Goodman Globe Union Incorporated 5757 North Green Bay Avenue Milwaukee, Wisconsin 53201	1	Dr. Charles H. Sherman Code TD 121 Naval Underwater Systems Center New London, Connecticut 06320	1
Professor Hatsuo Ishida Department of Macromolecular Science Case-Western Reserve University Cleveland, Ohio 44106	1	<del>Dr. William Risen Department of Chemistry Brown University Providence, Rhode Island 02192</del>	1
Dr. David Soong Department of Chemical Engineering University of California Berkeley, California 94720	1	Dr. Alan Gent Department of Physics University of Akron Akron, Ohio 44304	1
Dr. Curtis W. Frank Department of Chemical Engineering Stanford University Stanford, California 94305		Mr. Robert W. Jones Advanced Projects Manager Hughes Aircraft Company Mail Station D 132 Culver City, California 90230	1

TECHNICAL REPORT DISTRIBUTION LIST, 356A

<u>No.</u>	<u>Copies</u>	<u>No.</u>	<u>Copies</u>
Dr. C. Giori IIT Research Institute 10 West 35 Street Chicago, Illinois 60616	1	Dr. J. A. Manson Materials Research Center Lehigh University Bethlehem, Pennsylvania 18015	1
Dr. R. S. Roe Department of Materials Science and Metallurgical Engineering University of Cincinnati Cincinnati, Ohio 45221	1	Dr. R. F. Helmreich Contract RD&E Dow Chemical Co. Midland, Michigan 48640	1
Dr. Robert E. Cohen Chemical Engineering Department Massachusetts Institute of Technology Cambridge, Massachusetts 02139	1	Dr. R. S. Porter Department of Polymer Science and Engineering University of Massachusetts Amherst, Massachusetts 01002	1
Dr. T. P. Conlon, Jr., Code 3622 Sandia Laboratories Sandia Corporation Albuquerque, New Mexico	1	Professor Garth Wilkes Department of Chemical Engineering Virginia Polytechnic Institute and State University Blacksburg, Virginia 24061	1
Dr. Martin Kaufmann, Head Materials Research Branch, Code 4542 Naval Weapons Center China Lake, California 93555	1	Dr. Kurt Baum Fluorochem Inc. 6233 North Irwindale Avenue Azusa, California 91702	1
Professor S. Senturia Department of Electrical Engineering Massachusetts Institute of Technology Cambridge, Massachusetts 02139	1	Professor C. S. Paik Sung Department of Materials Sciences and Engineering Room 8-109 Massachusetts Institute of Technology Cambridge, Massachusetts 02139	1
Dr. T. J. Reinhart, Jr., Chief Composite and Fibrous Materials Branch Nonmetallic Materials Division Department of the Air Force Air Force Materials Laboratory (AFSC) Wright-Patterson AFB, Ohio 45433	1	Professor Brian Newman Department of Mechanics and Materials Science Rutgers, The State University Piscataway, New Jersey 08854	1
Dr. J. Lando Department of Macromolecular Science Case Western Reserve University Cleveland, Ohio 44106	1		
Dr. J. White Chemical and Metallurgical Engineering University of Tennessee Knoxville, Tennessee 37916	1		

TECHNICAL REPORT DISTRIBUTION LIST, GEN

<u>No.</u>	<u>Copies</u>	<u>No.</u>	<u>Copies</u>
Office of Naval Research Attn: Code 472 800 North Quincy Street Arlington, Virginia 22217	2	U.S. Army Research Office Attn: CRD-AA-IP P.O. Box 1211 Research Triangle Park, N.C. 27709	1
ONR Branch Office Attn: Dr. George Sandoz 536 S. Clark Street Chicago, Illinois 60605	1	Naval Ocean Systems Center Attn: Mr. Joe McCartney San Diego, California 92152	1
ONR Area Office Attn: Scientific Dept. 715 Broadway New York, New York 10003	1	Naval Weapons Center Attn: Dr. A. B. Amster, Chemistry Division China Lake, California 93555	1
ONR Western Regional Office 1030 East Green Street Pasadena, California 91106	1	Naval Civil Engineering Laboratory Attn: Dr. R. W. Drisko Port Hueneme, California 93401	1
ONR Eastern/Central Regional Office Attn: Dr. L. H. Peebles Building 114, Section D 666 Summer Street Boston, Massachusetts 02210	1	Department of Physics & Chemistry Naval Postgraduate School Monterey, California 93940	1
Director, Naval Research Laboratory Attn: Code 6100 Washington, D.C. 20390	1	Dr. A. L. Slafkosky Scientific Advisor Commandant of the Marine Corps (Code RD-1) Washington, D.C. 20380	1
The Assistant Secretary of the Navy (RE&S) Department of the Navy Room 4E736, Pentagon Washington, D.C. 20350	1	Office of Naval Research Attn: Dr. Richard S. Miller 800 N. Quincy Street Arlington, Virginia 22217	1
Commander, Naval Air Systems Command Attn: Code 310C (H. Rosenwasser) Department of the Navy Washington, D.C. 20360	1	Naval Ship Research and Development Center Attn: Dr. G. Bosmajian, Applied Chemistry Division Annapolis, Maryland 21401	1
Defense Technical Information Center Building 5, Cameron Station Alexandria, Virginia 22314	12	Naval Ocean Systems Center Attn: Dr. S. Yamamoto, Marine Sciences Division San Diego, California 91232	1
Dr. Fred Saalfeld Chemistry Division, Code 6100 Naval Research Laboratory Washington, D.C. 20375	1	Mr. John Boyle Materials Branch Naval Ship Engineering Center Philadelphia, Pennsylvania 19112	1

TECHNICAL REPORT DISTRIBUTION LIST, GEN

	<u>No.</u>
	<u>Copies</u>

Dr. Rudolph J. Marcus Office of Naval Research Scientific Liaison Group American Embassy APO San Francisco 96503	1
--	---

Mr. James Kelley DTNSRDC Code 2803 Annapolis, Maryland 21402	1
--	---

